Acta Biomaterialia 96 (2019) 505–516

Contents lists available at ScienceDirect

Acta Biomaterialia

journal homepage: www.elsevier.com/locate/actabiomat

Full length article

In vitro–in vivo correlation of inhalable budesonide-loaded large porous particles for sustained treatment regimen of asthma

Jiaqi Li [a], Huangliang Zheng [a], Lu Qin [a], En-Yu Xu [c], Linglong Yang [b], Lan Zhang [a], Xiaofei Zhang [a], Linlin Fan [b], Moritz Beck-Broichsitter [d], Uwe Muenster [d], Linc Chen [e], Yuyang Zhang [b,*], Shirui Mao [a,*]

[a] School of Pharmacy, Shenyang Pharmaceutical University, Shenyang 110016, China
[b] School of Life Science and Biopharmaceutics, Shenyang Pharmaceutical University, Shenyang 110016, China
[c] Department of Forensic Toxicological Analysis, School of Forensic Medicine, China Medical University, Shenyang 110122, China
[d] Chemical & Pharmaceutical Development, Bayer AG, D-42117 Wuppertal, Germany
[e] Chemical and Pharmaceutical Development, Bayer AG, Beijing 100020, China

ARTICLE INFO

Article history:
Received 7 April 2019
Received in revised form 20 June 2019
Accepted 27 June 2019
Available online 29 June 2019

Keywords:
In vitro drug release
IVIVC
Large porous particles
Lung delivery
Sustained release
Therapeutic efficacy
Systemic exposure

ABSTRACT

Large porous particles (LPPs) are well-known vehicles for drug delivery to the lungs. However, it remains uncertain whether or to which extent the *in vitro* drug release behavior of LPPs can be predictive of their *in vivo* performance (e.g., systemic exposure and therapeutic efficacy). With regard to this, three budesonide-loaded LPP formulations with identical composition but distinct *in vitro* drug release profiles were studied *in vivo* for their pharmacokinetic and pharmacodynamic behavior after delivery to rat lung, and finally, an *in vitro/in vivo* correlation (IVIVC) was established. All formulations reduced approximately 75% of the uptake by RAW264.7 macrophages compared with budesonide/lactose physical mixture and showed a drug release-dependent retention behavior in the lungs of rats. Likewise, the highest budesonide plasma concentration was measured for the formulation revealing the fastest *in vitro* drug release. After deconvolution of the plasma concentration/time profiles, the calculated *in vivo* drug release data were successfully utilized for a point-to-point IVIVC with the *in vitro* release profiles and the predictability of the developed IVIVC was acceptable. Finally, effective therapy was observed in an allergic asthma rat model for the sustained drug release formulations. Overall, the obtained *in vitro* results correlate well with the systemic drug exposure and the therapeutic performance of the investigated lung-delivered formulations, which can provide an experimental basis for IVIVC development in the pulmonary-controlled delivery system.

Statement of Significance

Large porous particles (LPPs) are well-known vehicles for drug delivery to the lungs. However, it remains uncertain whether or to which extent the *in vitro* drug release behavior of LPPs can be predicted by their *in vivo* performance (e.g., systemic exposure and therapeutic efficacy). With regard to this, three budesonide-loaded PLGA-based LPP formulations with identical composition but distinct *in vitro* drug release profiles were studied *in vivo* for their pharmacokinetic and pharmacodynamic behavior, and finally, an *in vitro/in vivo* correlation (IVIVC) was established. It was demonstrated that the influence of the *in vitro* drug release profile was obvious during lung retention, systemic exposure, and therapeutic efficacy measurements. An IVIVC (Level A) was successfully established for the budesonide-loaded LPPs delivered to the airspace of rats for the first time. Taken together, the present work will clearly support research and development activities in the field of controlled drug delivery to the lungs.

1. Introduction

Asthma is an intricate respiratory disease characterized by airway inflammation, mucus hypersecretion, and acute hyper-responsiveness [1]. It is reported that approximately 334

* Corresponding authors at: School of Pharmacy, Shenyang Pharmaceutical University, 103 Wenhua Road, 110016 Shenyang, China.
E-mail addresses: 13614053862@163.com (Y. Zhang), maoshirui@syphu.edu.cn (S. Mao).

https://doi.org/10.1016/j.actbio.2019.06.056
1742-7061/

million people worldwide are suffering from this chronic airway disease, and this figure will increase up to 400 million by the year 2025 [2]. The direct/targeted administration of medications to the lungs by inhalation represents a promising strategy for the treatment of respiratory diseases. To increase patients' convenience, it would be highly desirable to maintain "effective" drug concentrations in the lungs for a prolonged period of time [3]. However, presently, most inhalation products on the market are short-acting dosage forms, which require frequent dosing. Another evident disadvantage with current medications is their undesired pharmacokinetic profile, showing peak concentrations immediately after inhalation (with chance for adverse events) followed by a prompt decline (short duration of action) [4].

To achieve a sustained therapeutic effect within the lungs, a variety of formulation strategies such as large porous (micro)particles (LPPs) have been proposed [5,6]. Characterized by their large geometric diameter (>5 μm) and porous structure (bulk density of <1 g/cm^3), LPPs evade macrophage phagocytosis while maintaining a suitable aerodynamic behavior. For example, it was previously shown by our group that LPPs prepared from poly (lactide-*co*-glycolide) (PLGA) served as a controlled drug delivery system, demonstrating a sustained therapeutic effect within the lungs for up to 4 h [7]. However, it remains uncertain to which extent the *in vitro* drug release behavior is predictive of therapeutic efficacy *in vivo*. With regard to this, the establishment of a valid *in vitro*/*in vivo* correlation (IVIVC) is desirable to allow for prediction of a therapeutic effect and dosing interval from a rather simple *in vitro* characterization.

The objective of our present study was to investigate the *in vitro* drug release behavior and *in vivo* performance of budesonide-loaded LPPs with distinct *in vitro* drug release rates after delivery to the lung. After a thorough physicochemical characterization, the influence of the *in vitro* drug release rates on the *in situ* lung retention, pharmacokinetic behavior, and *in vivo* therapeutic effect was investigated in rats. Fitting equations for IVIVC could be established from the obtained *in vitro* drug release and lung retention/pharmacokinetic data. This report correlates the *in vitro* drug release with retention, systemic exposure, and therapeutic efficacy of lung-delivered LPPs, which could provide a correlation database for the design and development of controlled drug release medication intended for the administration to the respiratory tract.

2. Materials and methods

2.1. Materials

PLGA (Resomer® RG 503H) was purchased from Evonik (Germany). Micronized budesonide was acquired from Hubei Gedian Humanwell Pharmaceutical Co. Ltd. (China). Lactohale® 200 was received as a gift from DFE Pharma (China). Poly(vinyl alcohol) (PVA 205) and poly(vinyl pyrrolidone) (PVP-k12) were donated by Kuraray Trading Co., Ltd. (Japan) and International Specialty Products Inc. (USA), respectively. Pulmicort® Turbuhaler® (AstraZeneca, UK) was purchased from a local pharmacy. Phosphate-buffered saline (PBS) solution was purchased from Dalian Meilun Biotechnology Co., Ltd (Dalian, China). High-pressure liquid chromatography (HPLC)-grade methanol and dichloromethane (DCM) were supplied by Shandong Yuwang Co., Ltd. (China). Ovalbumin (OVA) was purchased from Sigma-Aldrich (USA). Pentobarbital sodium was obtained from Applichem (Germany). Wright-Giemsa and Hematoxylin-Eosin staining solutions were supplied by Wanleibio (China) and Jiancheng (China), respectively. Rat IL-4 and IL-5 ELISA kits were obtained from Cusabio (China). TRIzol® reagent was bought from Ambion (USA). MasterMix Kit (abm®) and EvaGreen 2X qPCR MasterMix (abm®) were purchased from Takara Bio (China). All other reagents, unless otherwise specified, were of analytical grade and used as received.

2.2. Preparation of budesonide-loaded LPPs

2.2.1. Emulsion solvent evaporation (ESE) method

Budesonide-loaded LPPs (LPP-1 and LPP-2) were prepared by a modified single emulsion (O/W) solvent evaporation method as described previously [7]. Briefly, 66.7 mg budesonide were dissolved in 3 ml of DCM together with 600 mg of PLGA and 90 mg of PVP. Then, the resulting organic phase was injected into 300 ml (LPP-1) or 500 ml (LPP-2) of aqueous phase containing 0.5% (w/v) of PVA under high-speed homogenization (Ultra-Turrax® T25, IKA, Germany) for 30 s. The final emulsion was subsequently stirred to evaporate the DCM under a water bath at 25 °C for 4 h. The obtained LPPs were collected by centrifugation at 2000 rpm for 5 min, washed three times with distilled water, and finally freeze-dried (FDU-1100, Tokyo Rikakikai Co., Ltd, Japan) for 24 h.

2.2.2. Premix membrane emulsification (PME) method

Budesonide-loaded LPPs (LPP-3) were prepared by the PME method [8], using the same procedure as that for LPP-1. Briefly, budesonide (66.7 mg), PLGA (600 mg), and PVP (90 mg) were dissolved together in 3 ml of DCM. The resulting oil phase was injected into 50 ml of aqueous phase containing 0.5% (w/v) PVA under high-speed homogenization for 30 s. Next, by using a Shirasu-porous-glass (SPG) emulsification kit (SPG Technology Co., Ltd, Japan), the pre-emulsion (stored in a pressure-tight vessel) was passed through a SPG membrane (tube-shaped with an outer diameter of 10 mm) with pore size of 15 μm under nitrogen gas pressure of 0.065 MPa for three times. The obtained emulsion was rapidly added to 250 ml of aqueous phase containing 0.5% (w/v) PVA. The final emulsion was subsequently stirred to evaporate the DCM under a water bath at 25 °C for 4 h. The cleaning and drying processes were identical as outlined above.

2.3. Characterization of budesonide-loaded LPPs

2.3.1. Particle size measurement

The geometric particle size (i.e., the volumetric median diameter [$D_{v,50}$]) of the budesonide-loaded LPPs was determined by laser diffraction (Beckman-Coulter, LS 230, USA). The span value was calculated as follows:

$$\text{Span} = \frac{D_{v,90} - D_{v,10}}{D_{v,50}}$$

2.3.2. Drug loading

The loading content of budesonide in the LPPs was tested according to the following procedure: 10 mg of LPPs were weighed precisely and then dissolved in 1 ml of DCM, which was further diluted to 50 ml with methanol. The mixture was centrifuged at 10,000 rpm for 10 min. A sample from the supernatant was subsequently subjected to HPLC analysis. Agilent 1260 Infinity HPLC equipment (Agilent Technologies Inc., USA) was used, and the analysis was conducted on an Agilent Zorbax SB C_{18}-H column (150 mm × 4.6 mm, particle size: 5 μm) (Agilent Technologies Inc., USA) equipped with a ColumnShield™ ACE-HP205 pre-column (Guangzhou FLM Scientific Instrument Co., Ltd, China) at 40 °C. The detection wavelength was 248 nm and drug retention time was in the range of 5.1–5.2 min (mobile phase: water/methanol (28/72, v/v); flow rate: 1 ml/min). Under the above-mentioned chromatographic conditions, the limit of detection (LOD) was found to be 0.05 μg/ml, and the limit of quantitation (LOQ) was

0.15 μg/ml. The linearity of drug concentration to peak area was good in the range of 0.50–40.00 μg/ml (A = 21.109C-4.3517 (R^2 = 0.9999)). The precision and recovery met the requirements for *in vitro* analysis. The drug loading (DL) percent is defined in the following equation:

$$DL\% = \frac{M_{\text{actual drug loaded}}}{M_{\text{dosage form weighed}}} \times 100\%$$

2.3.3. Scanning electron microscopy

The morphology of the budesonide-loaded LPPs was observed using a scanning electron microscope (S-3400N, Hitachi, Japan). For surface morphology observation, a small amount of powder sample was sprinkled onto a double-sided adhesive conductive tape attached to a copper stub and then sputter-coated with gold under vacuum. The images were captured with an accelerating voltage of 25 kV. A frozen section was prepared for particle cross-section observation. Drug powders were soaked in an aqueous solution containing 20% gelatin-5% glycerin for 3 h at 37 °C. After solidification by storing in −20 °C, the microspheres coated with gelatin–glycerin jelly were frozen in liquid nitrogen for 5 min and cryo-sectioned. The prepared frozen sections were then placed on the copper stub and sputter-coated with gold under vacuum. The images were captured at an accelerating voltage of 15 kV.

2.4. In vitro drug release

To evaluate the *in vitro* release behavior of budesonide from the LPPs, ~2.50 mg of drug-loaded LPPs were weighed precisely and dispersed into 5 ml of phosphate buffer (10 mM, pH 7.3) in a centrifuge tube. Sodium dodecyl sulfate (0.15% (w/v)) was added for solubilization, and the solubility of budesonide in the medium was 175.3 μg/ml (sink condition). The dispersion was continuously incubated in an air-bath oscillator (THZ-92B, Shanghai Boxun Co., Ltd, China) at 37 (±1) °C with a speed of 80 rpm. At predetermined time points (2, 4, 8, 12, 24, 36, 48, and 72 h), the release medium was collected, and after centrifugation, the supernatant was analyzed for the drug content by HPLC. Thereafter, LPPs were re-suspended in fresh media of equal volume and further incubated.

The same procedure was followed for incubation of drug in the release medium to observe particle morphology during the process of drug release. At specific time points (4, 12, and 24 h), the powder sample was washed with distilled water and centrifuged for collection. After freeze-drying, scanning electron microscopy was performed for capturing the particle surface morphology as mentioned in Section 2.3.3.

2.5. In vitro aerodynamic performance

The *in vitro* aerodynamic properties of the LPPs were investigated using a Next Generation Impactor (NGI, Copley Scientific, UK) according to the U.S. pharmacopeia on aerosols as reported previously [7]. Before making measurements, the pre-separator attachment and all the impactor plates were pre-coated with 10% (w/v) Tween 20 in ethanol solution. The powder (20 mg) was weighed precisely and loaded into one capsule (No. 3 HPMC capsule, Capsugel®, Suzhou, China). A Cyclohaler® DPI device (Teva Pharmaceuticals, The Netherlands) was used for drug inhalation. When actuated, the particles were deposited in/on each compartment/stage, which were then rinsed with DCM and collected with methanol. The budesonide concentration was analyzed by HPLC, and the drug amount (m) was calculated. The experimental mass median aerodynamic diameter ($MMAD_e$) was provided by bundled NGI software (Copley Scientific, UK) and the fine particle fraction (FPF%) was calculated by the following equation:

$$FPF\% = \frac{m_{stage\ 1-7}}{m_{total(induction\ port+pre-separator+all\ stages)}} \times 100\%$$

2.6. Macrophage uptake study

Murine RAW264.7 macrophages (ATCC TIB-71, USA) were seeded in 6-well plates at a density of 5×10^5 cells/ml and incubated in Dulbecco's Modified Eagle Medium (DMEM) supplemented with 10% fetal bovine serum at 37 °C, 5% CO_2 for 24 h. Thereafter, the cells were washed with DMEM three times. LPP-1, -2, and -3 and the physical mixture (budesonide/Lactohale® 200 (5:95)) were uniformly dispersed in 1 ml of the medium (~80 μg of budesonide per formulation) before incubating with the RAW264.7 cells. At specific time points (2, 4, 8, and 12 h), the medium was removed, the incubated cells were washed three times with phosphate buffer and then lysed using 500 μl of radioimmuno-precipitation lysis buffer for 30 min. Thereafter, 300 μl of the lysed cell solution was mixed with an equal amount of dimethyl sulfoxide and then centrifuged. The supernatant was analyzed for drug content by HPLC. The rest of the sample was centrifuged, and 10 μl of the supernatant was used to quantify the protein content using a BCA assay kit. The final cell uptake was calculated according to the following equation:

$$\text{Celluptake} = \frac{M_{\text{budesonide}}}{M_{\text{protein}}} (\mu g/\text{mg protein})$$

2.7. Animals

Male Sprague Dawley rats (~200 g) were purchased from the Laboratory Animal Center of Shenyang Pharmaceutical University. Rats were housed under conditions of temperature at 23 ± 3 °C with a relative humidity of 55 ± 10% and a 12 h light–dark cycle. All the procedures were in compliance with ethical standards and guidelines issued by the ethics committee and Shenyang Pharmaceutical University for the care and use of laboratory animals (approval number: SYPU-IACUC-C2018-10-8-205).

2.8. In vivo retention study

The residence behavior of drug-loaded LPPs was analyzed after intra-tracheal powder insufflation to rats as previously described [9]. Initially, rats were intraperitoneally anesthetized with 4.0% (w/v) chloral hydrate at a dose of 7.0 ml/kg, and the LPP-1, -2, and -3 formulations (the physical mixture (budesonide/Lactohale® 200 (5/95)) served as a control) were delivered to the airspace of 4 rats per group using a DP-4 Dry Powder Insufflator™ (Penn-Century, USA). At predetermined time points (0, 2, 4, 8, and 12 h), the rats were sacrificed using a cervical dislocation maneuver, and the trachea was dissected. Subsequently, 2 ml of dimethyl sulfoxide was injected into the lungs and re-aspirated after 30 s. This procedure was repeated three times. One milliliter of the pooled bronchoalveolar lavage fluid (BALF) was mixed with 2 ml of methanol to precipitate the proteins. The mixture was homogenized and then centrifuged at 10,000 rpm for 10 min. The supernatant was analyzed by HPLC.

2.9. In vivo pharmacokinetic study

The plasma concentration/time profiles (systemic exposure) of budesonide were followed after formulation application to the lungs of rats. Again, LPP-1, -2, and -3 formulations (the physical

mixture (budesonide/Lactohale® 200 (5:95)) served as a control) were delivered to the airspace of 6 rats per group as outlined above. The entire administration dose was equivalent to 350 μg of budesonide per kg of animal body weight. After formulation application, blood samples were collected at predetermined time points (5, 15, and 30 min and 1, 1.5, 2, 3, 4, and 6 h) through the *retro*-orbital sinus (sodium heparin was used as the anticoagulant). Blood samples were centrifuged at 4,500 rpm for 10 min to isolate the plasma, which was stored at −20 °C until further analysis.

Budesonide plasma concentrations were determined by LC–MS [10]. Briefly, 100 μl of triamcinolone acetonide (60 ng/ml) was added as an internal standard, after which budesonide was extracted from 100 μl of plasma with 200 μl of acetonitrile. After vortexing for 5 min and centrifugation at 13,000 rpm for 10 min, the final supernatant was used to determine the drug concentrations using an Agilent 1260–6420 tandem triple-quadrupole LC-MS/MS equipment. An Agilent Zorbax SB C18 column (2.1 mm × 50 mm, 1.8 μm) was used for separation. The mobile phase was acetonitrile/0.1% formic acid (50/50 (v/v)) with a flow rate of 0.2 ml/min. The injection volume was 1 μl, and the positive-ion mode was used as the ESI ionization source. Peak area ratios between calibration samples and internal standards were plotted against their concentrations, achieving a good linearity with R^2-value of 0.999 in the range of 0.02–1.00 μg/ml. The obtained plasma concentrations of budesonide were then used to calculate the pharmacokinetic parameters (DAS.2.0 software, Mathematical Pharmacology Professional Committee, China).

2.10. Establishing IVIVC

In this study, Level A (point-to-point) correlation between the *in vitro* release profiles and the *in vivo* dissolved fractions was established for the distinct LPP formulations (i.e., LPP-1, -2, and -3) according to FDA recommendation on IVIVC study [11]. The *in vivo* dissolution [input, *I(t)*] was the key point for IVIVC establishment. If the *in vivo* property of the reference immediate-release dosage form (physical mixture of budesonide/Lactohale® 200 (5/95)) was regarded as a weight function [weighting, *W(t)*], then the other delayed behaviors (sustained dosage forms) could be viewed as a result of the superposition of small-dose weight functions at different time points *in vivo*, that is, the response function [response, *R(t)*] derived from *in vivo* plasma concentration/time data. The three functions constituted the relationship as shown in Scheme 1.

The mathematical relationship of the three functions is shown below:

$$R(t) = \int_0^t I(\gamma)W(t-\gamma)d\gamma$$

The *in vivo* dissolution [input, I(t)] was obtained by deconvoluting the above formula using the IVIVC Toolkit of Phoenix WinNonlin® (v.6.4, Pharsight, USA). Thereafter, the *in vivo* dissolution/absorption was correlated with the *in vitro* release at identical time intervals by a linear regression method for the three LPPs.

Furthermore, a combination of two LPPs was used for the correlation according to the above procedures to establish a fitting formula, which was then applied to predict the *in vivo* dissolution/absorption of the third LPP formulation based on its *in vitro* release profile. The convolution method was utilized to obtain the predicted *in vivo* plasma concentration from the predicted *in vivo* dissolution/absorption profile, by which predictability validation could be evaluated. The predictability validation was concentrated on estimating the percent of prediction error (PE%) between the observed and predicted plasma concentration profiles (AUC, C_{max}), according to the formula:

$$PE\% = \frac{AUC_{tested} - AUC_{predicted}}{AUC_{tested}} \times 100\%$$

$$PE\% = \frac{Cmax_{tested} - Cmax_{predicted}}{Cmax_{tested}} \times 100\%$$

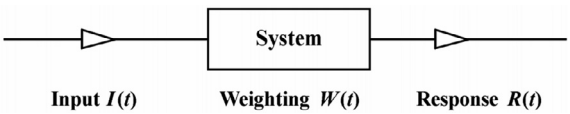

Scheme 1. Illustration of input, weighting, and response functions *in vivo* [12].

2.11. In vivo pharmacodynamics study

2.11.1. Allergic asthma rat model and treatment

The allergic asthma rat model was established according to the method reported previously with minor modifications [13,14]. Briefly, each rat was sensitized twice with an intraperitoneal injection of a mixture containing 100 mg of ovalbumin (OVA) and 200 mg of aluminum hydroxide in phosphate buffer (1 ml) on days 0 and 7, respectively. One week later, the rats were consecutively (once daily) challenged with an aerosol of 2% (w/v) OVA using a jet nebulizer for 13 days. Then, the rats were randomly divided into six groups consisting of five animals in each group: control group (no OVA challenge, no drug treatment); model group (OVA challenge only); budesonide-loaded LPP-1, -2, and -3 groups; and the physical mixture group (budesonide/Lactohale® 200 (5/95)). All experimental groups were administered (budesonide 87.5 μg/kg rat) once every three days using a dry powder insufflator (DP-4, Penn-Century, USA) before OVA irritation. On day 27, the rats were euthanized and their bronchoalveolar fluid (BALF) and lung tissues were collected for further analysis (Scheme 2).

2.11.2. BALF and cellular differential counts

To obtain BALF, the trachea and the lung lobes were isolated. The right bronchi were ligatured, and the left lobes were lavaged three times with phosphate buffer. The lavage fluid was centrifuged at 1000 rpm for 10 min at 4 °C, and the obtained supernatants were stored at −80 °C for cytokine examination. The cell pellet was re-suspended with 1 ml of phosphate buffer for total cell count using a hemocytometer and then smeared on a glass slide for Wright–Giemsa staining for differential cell counts.

2.11.3. Measurement of cytokines in BALF

The levels of cytokine (i.e., IL-4 and IL-5) in BALF were determined using ELISA kits according to the manufacturer's instructions.

2.11.4. Real-time-PCR for IL-4 and IL-5 mRNA expression in lung tissues

After recovery of BALF, the samples from left lobes were stored at −80 °C for real-time PCR (RT-PCR) analysis of gene expression. Briefly, total RNA was extracted from lungs using the TRIzol® reagent according to the manufacturer's protocol, and then the reverse transcription reaction was performed using the 5X All-In-One RT MasterMix Kit (abm®) in an RNase-free environment for cDNA synthesis. The target genes were determined by RT-PCR using SYBR Premix Ex Taq. The PCR protocol consisted of 10 min at 95 °C followed by 33 cycles of 15 s at 95 °C and 60 s at 60 °C. The primer sequences used for quantification are shown in Table 1. The relative expression of the target gene was calculated using the comparative $2^{-\Delta\Delta Ct}$ method [15].

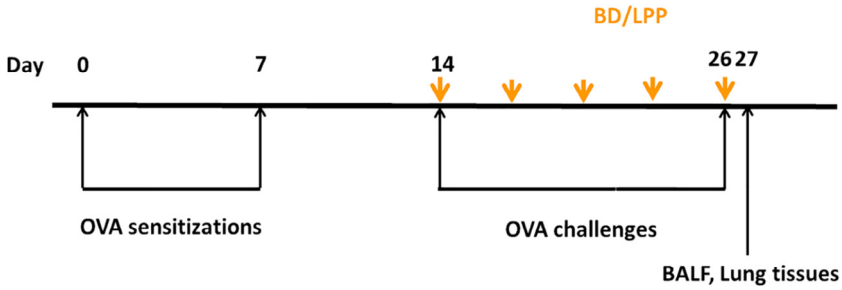

Scheme 2. Experimental protocol describing the OVA-induced allergic asthma rat model used for drug treatment.

Table 1
Primer sequence.

Gene		Oligonucleotides
β-Actin	Forward	5′-TTGCTGACAGGATGCAGAAG-3′
	Reverse	5′-CAGTGAGGCCAGGATAGAGC-3′
IL-4	Forward	5′-TGATGTACCTCCGTGCTTGA-3′
	Reverse	5′-CAGTGTTGTGAGCGTGGACT-3′
IL-5	Forward	5′-TGAGGATGCTTCTGTGCTTG-3′
	Reverse	5′-AGAGCTCGGTGAGTGGACAG-3′

2.11.5. Lung histopathology

The right lobes of rats (which were not lavaged) were excised, fixed with 10% formalin for 48 h, embedded in paraffin after alcohol gradient treatment, and sliced into 5 μm thin sections for hematoxylin-eosin staining. The inflammatory cell infiltrate was observed using a light microscope (IX71, Olympus, Japan) at a magnification of 100X as previously described [16]. Briefly, inflammation score was designated as none (score, 0), mild (score, 1–2), moderate (score, 3–4), or severe (score, 5–6) inflammation, which was done blinded. The final score was calculated by addition of scores for both peribronchial and perivascular inflammation. The captured images were analyzed using ImageJ software to determine the thickness of airway walls.

2.12. Statistical analysis

In vitro data are presented as the mean ± standard deviation (SD) from at least three independent measurements. *In vivo* data are expressed as mean ± standard error of means (SEM) from at least four independent measurements. Statistical analysis was performed using Prism 5 (GraphPad Software, USA) by one-way ANOVA. A probability value of $p < 0.05$ was considered statistically significant.

3. Results

3.1. Preparation and characterization of budesonide-loaded LPPs

Changing the O/W phase ratio during the manufacturing of LPPs by the solvent evaporation process (with PLGA as the matrix polymer and PVP as pore former) was reported to have a tremendous influence on the resulting release profile of the embedded drug [17]. As outlined in Table 2, three budesonide-loaded LPP formulations with distinct physicochemical properties were obtained and characterized. Under application of the ESE method, an O/W phase ratio of 3:300 (LPP-1) led to the formation of LPPs with a particle size of (~20 μm) and a tap density of <0.3 g/ml. By contrast, an O/W phase ratio of 3:500 (LPP-2) formed smaller particles (~12 μm) with a higher density (>0.4 g/ml). Application of the PME method (LPP-3) resulted in the smallest particles (~9 μm) with a tap density of ~0.38 g/ml.

As shown in Fig. 1, scanning electron microscopy analysis of the three LPP formulations generally confirmed the size results presented in Table 2. Furthermore, comparison of the internal particle morphology/porosity underlined the determined tap densities [18]. LPPs with the highest porosity (LPP-1) showed the smallest tap density, and the tap density of LPP-2 was larger than that of LPP-3 owing to lower porosity.

The *in vitro* budesonide release rates from LPP-1, -2, and -3 differed significantly (Fig. 2). A remarkable burst release of ~30% within the first 2 h of incubation was detected for LPP-1, followed by a sustained release of budesonide during the next 70 h. For LPP-2, the burst release disappeared. Instead, a sustained and almost linear release profile was achieved during 72 h. Similarly, the burst release was not detectable for LPP-3 (prepared by the PME method), but a prolonged drug release over 72 h was observed. These results were in general agreement with the observation from scanning electron microscopy (Fig. 1), implying that LPP formulations with a lower porosity (LPP-2 < LPP-3 < LPP-1) led to a slower release of the encapsulated drug (LPP-2 < LPP-3 < LPP-1).

The morphology of the LPP formulations changed during the time-course of incubation (Fig. 3). After 4 h, the pore number and pore size on the surface of LPP-1 were larger than those of the other two formulations, which was in good agreement with its drug release profile (i.e., high burst release). By contrast, only a small amount of tiny pores was found on the surface of LPP-3. No pores were detected on the surface of LPP-2 after 4 h of incubation. After 12 h, larger pores appeared on LPP-1, and LPP-3 became more corrugated than LPP-2. After 24 h, all three formulations became wrinkled and porous to a comparable extent.

Table 2
Physicochemical properties of the utilized budesonide-loaded LPPs. Values are presented as the mean ± SD ($n = 3$).

Formulation	Preparation method	O/W phase ratio (v/v)	Particle size [μm] (span value)	Tap density [g/ml]	Drug loading [%]	$MMAD_e$ [μm]
LPP-1	ESE	3:300	$20.1 \pm 0.2^{\#,\&}$ (1.71)	$0.26 \pm 0.01^{\#,\&}$	6.0	3.6 ± 0.1
LPP-2	ESE	3:500	$12.6 \pm 0.1^{*,\&}$ (1.11)	$0.43 \pm 0.02^{*,\&}$	7.3	3.4 ± 0.3
LPP-3	PME	3:300	$9.2 \pm 0.1^{*,\#}$ (0.95)	$0.38 \pm 0.01^{*,\#}$	8.0	3.7 ± 0.1

Values are presented as the mean ± SD ($n = 3$). Statistically significant difference:
* $p < 0.05$ compared to LPP-1,
$^{\#}$ $p < 0.05$ compared to LPP-2,
$^{\&}$ $p < 0.05$ compared to LPP-3.

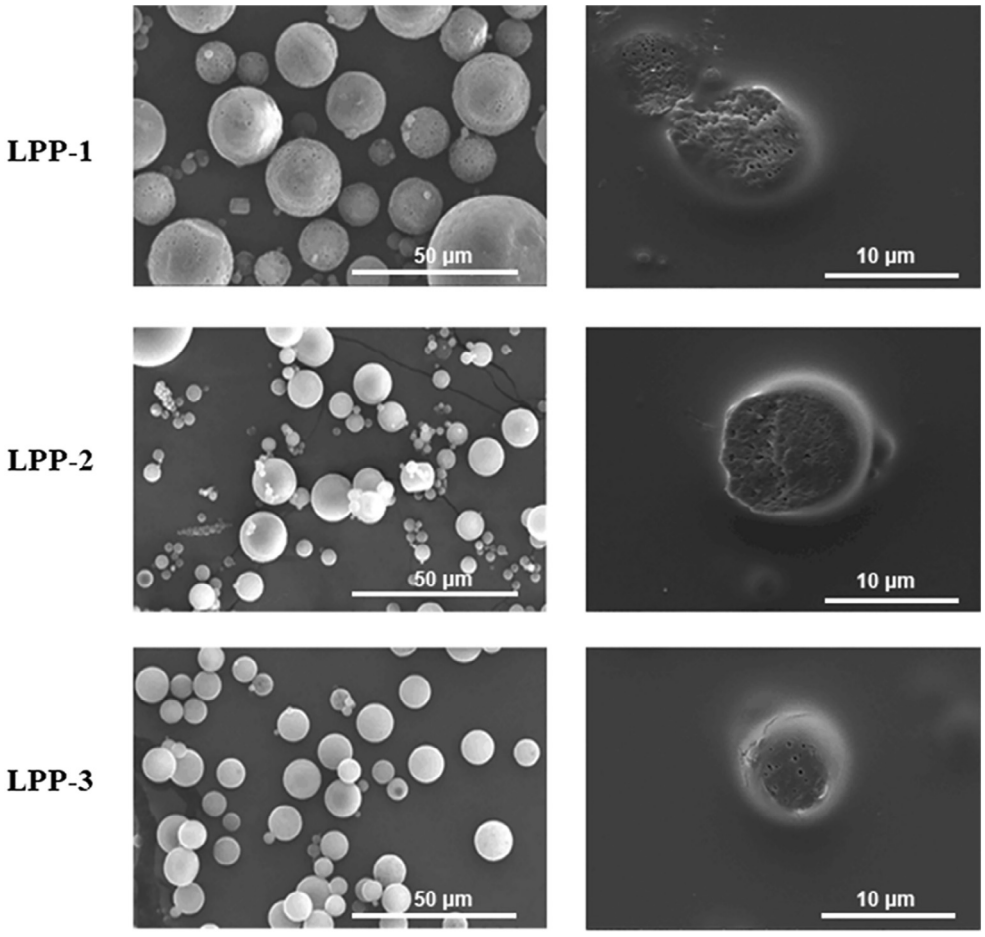

Fig. 1. Morphology characteristics of the utilized budesonide-loaded LPPs (left column: surface morphology, right column: cross-sections).

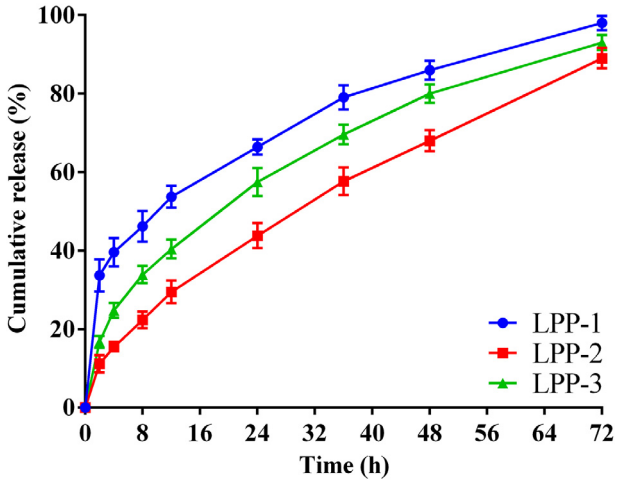

Fig. 2. *In vitro* drug release profiles of budesonide-loaded LPPs in phosphate buffer supplemented with 0.15% (w/v) sodium dodecyl sulfate (pH 7.3) (sink condition). Values are presented as the mean ± SD ($n = 3$).

3.2. In vitro aerodynamic properties of LPPs

The aerodynamic properties of the LPPs were evaluated and compared. As shown in Fig. 4, the three formulations displayed comparable aerodynamic diameter distributions (Stages 1–7), indicating a similar deposition zone in the lungs. In addition, experimental mass mean aerodynamic diameters ($MMAD_e$) were calculated according to the aerodynamic diameter distributions, and the results are shown in Table 2. All the three formulations showed suitable aerodynamic properties for inhalation with $MMAD_e$ values of <4 μm and FPF% values >20% [19]. Data implied that all the LPPs with different particle sizes had comparable deposition properties.

3.3. Macrophage uptake

Before the *in vivo* studies, the ability of the LPP formulations to evade macrophage phagocytosis was tested. For this purpose, LPP-1, 2, and 3 were incubated with RAW264.7 macrophage cells, and a physical mixture (budesonide/Lactohale® 200 (5/95)) was used as a control. It was found that the physical mixture was rapidly phagocytized by macrophages (Fig. 5). The increase in intracellular budesonide concentration caused by passive diffusion of the dissolved drug can be neglected owing to the low solubility of budesonide in the cell culture medium. In contrast, all the LPPs investigated could reduce the macrophage uptake significantly ($p < 0.05$) for up to 12 h, and nearly 75% decrease in uptake was observed when compared with the physical mixture group. No statistical difference in macrophage uptake was found among the LPPs investigated.

3.4. In vivo retention of budesonide-loaded LPPs

When the physical mixture (budesonide/lactose blend) was delivered to the airways of rats, a rapid decline in drug

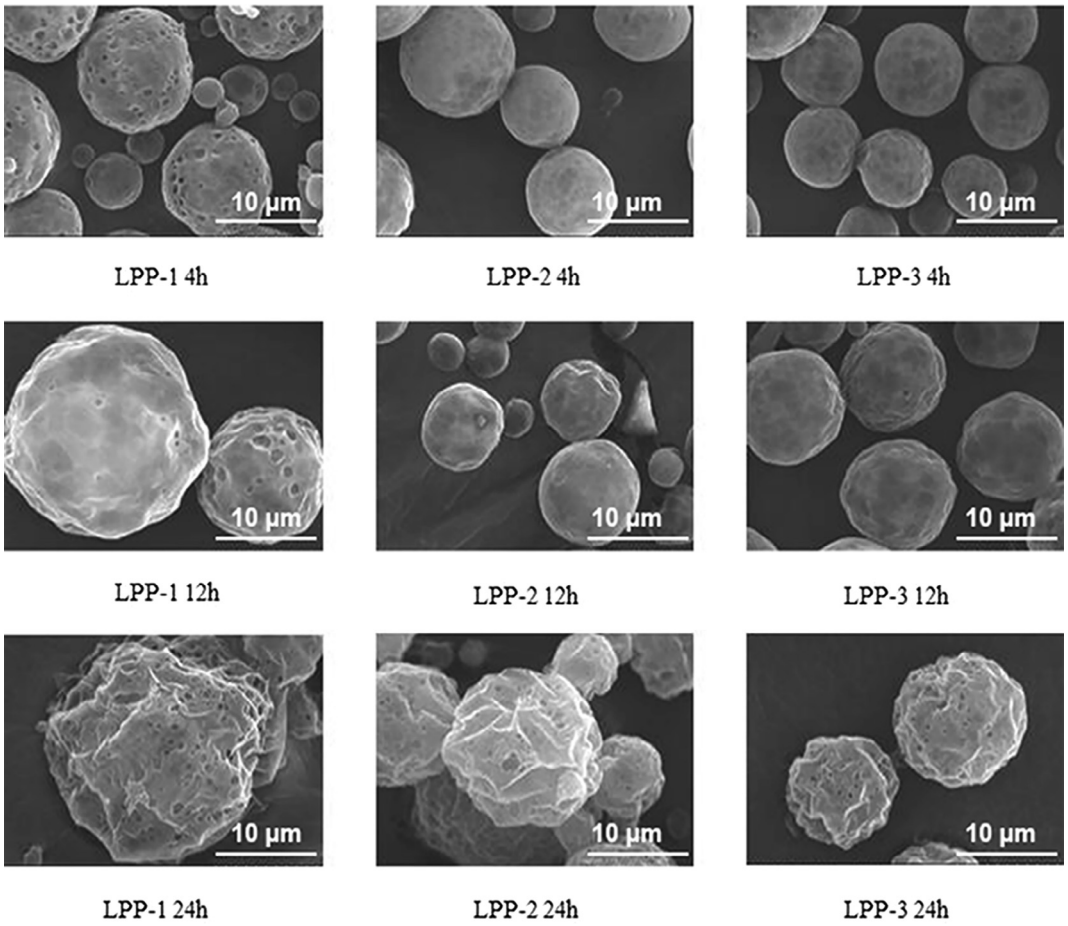

Fig. 3. Morphology of the utilized budesonide-loaded LPPs during the *in vitro* drug release experimentation.

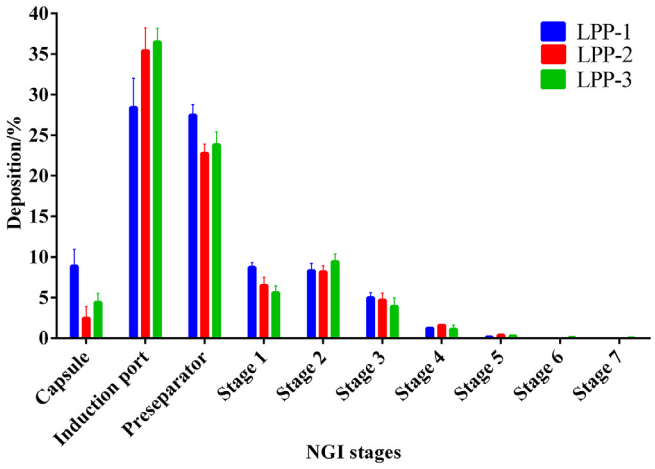

Fig. 4. *In vitro* aerodynamic particle size distribution of budesonide-loaded LPPs measured by NGI. Values are presented as the mean ± SD ($n = 3$).

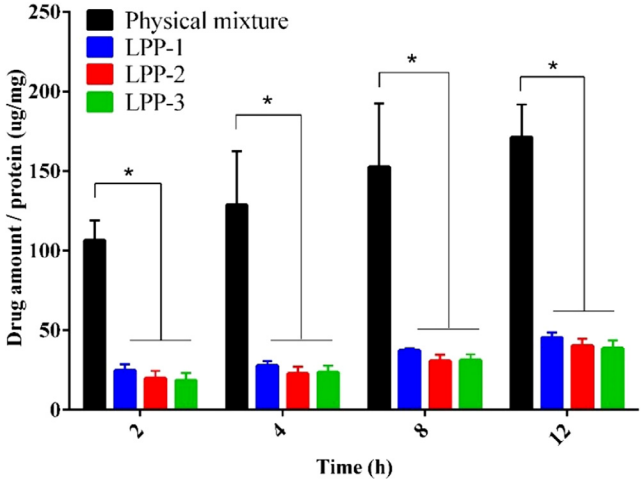

Fig. 5. Uptake of budesonide by RAW264.7 macrophages from drug-loaded LPP formulations and the physical mixture (budesonide/Lactohale® 200 (5/95)). Values are presented as the mean ± SD ($n = 3$). The asterisks indicate a statistically significant difference ($p < 0.05$).

concentration in the BALF was detected, with no measurable content already after 4 h (Fig. 6). By contrast, all LPP formulations displayed a prolonged retention in the lungs, which was in general agreement with the findings from the macrophage uptake study (Fig. 5). Compared to LPP-2 and LPP-3, LPP-1 showed a lower drug residual at each time point, which was associated with the rapid drug release behavior (Fig. 2).

3.5. In vivo pharmacokinetics of budesonide-loaded LPPs

The budesonide concentration in the plasma and the calculated pharmacokinetic parameters after intratracheal administration of the distinct LPP formulations were studied and compared with those of the physical mixture (budesonide/lactose blend) (Fig. 7,

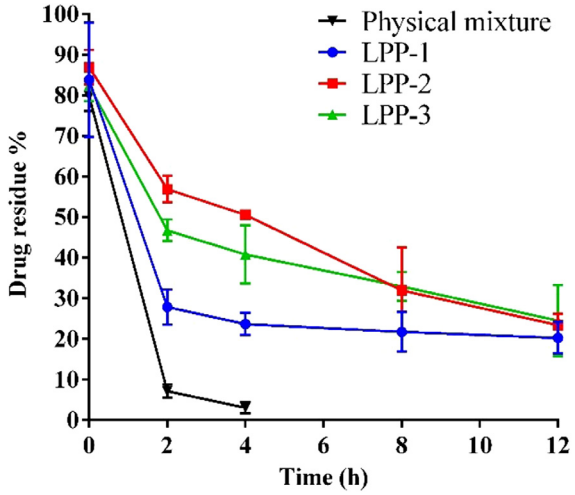

Fig. 6. *In vivo* residence time of lung-delivered, budesonide-loaded LPP formulations. The physical mixture (budesonide/Lactohale® 200 (5/95)) served as a control. Values were presented as the mean ± SEM (n = 4).

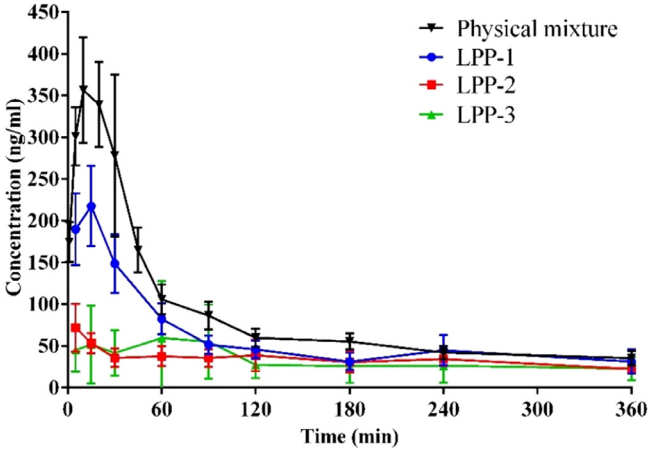

Fig. 7. Plasma concentration–time curves of budesonide after delivery of budesonide-loaded LPP formulations to rat lungs. The physical mixture (budesonide/Lactohale® 200 (5/95)) served as a control. Values were presented as the mean ± SEM (n = 6).

Table 3). LPP-1, -2, and -3 showed significantly lower systemic exposure of drug as evidenced by the C_{max} and $AUC_{0\text{-}t}$ when compared with the physical mixture group. The systemic drug concentration after delivery of LPP-1 to the lungs was significantly higher than those in the LPP-2 and LPP-3 groups ($p < 0.01$). Compared with the LPP-1 group, LPP-2 administration led to a 3.7- and 1.7-fold reduction in C_{max} and $AUC_{0\text{-}t}$, respectively (2.9- and 1.6-fold reduction of LPP-3). Thus, to decrease the extent of systemic drug exposure (and potential side effects), it is essential to control the burst release behavior of budesonide-loaded LPPs.

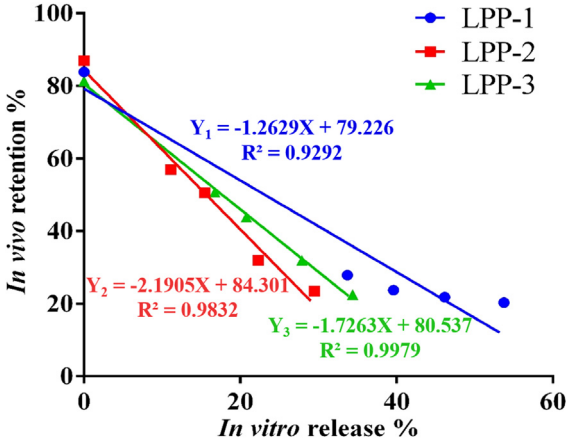

Fig. 8. Point-to-point comparison of the fraction released *in vitro* vs. fraction retained *in vivo* for three budesonide-loaded LPP formulations. The straight lines represent linear fits of the experimental data.

3.6. IVIVC evaluation

The *in vivo* performance is the sole criterion for pharmaceutical development [20]. On the one hand, the residence time in the target organ plays a vital role in prolonged drug therapy, and thus, a correlation between the *in vitro* drug release and *in vivo* retention of LPP formulations was established. As shown in Fig. 8, good/linear correlations were achieved for LPP-1, -2, and -3 (R^2 values > 0.90). The slopes were greater than 1, indicating that the decline in retention in the lungs was faster than the *in vitro* release.

On the other hand, systemic exposure is a reflection of the drug released from the deposited formulations in the lungs. Then the *in vitro* (drug release) and *in vivo* (deconvoluted from the plasma concentration/time data) concentrations were plotted against each other at different time points, and an appropriate line was fit to the data (Fig. 9). Linear correlations between the *in vitro* drug release percentage and the *in vivo* absorbed fraction were successfully established for LPP-1, -2, and -3 (R^2 > 0.99). The slope of the LPP-2 group was closest to 1, implying that LPP-2 exhibited the best consistency of the *in vitro* release to *in vivo* dissolution/absorption.

Level A IVIVCs developed by combining any two of the three formulations (LPP-1, -2, and -3) are shown in Fig. 10. Point-to-point linear relationships of the *in vitro* release and *in vivo* absorption were well established for all combinations, with fitting coefficients (R^2) greater than 0.90. Thereafter, the obtained fitting equation of a combination (e.g., LPP-2 and LPP-3) was used to predict the *in vivo* absorption of the other formulation (LPP-1) that was not included in the developed IVIVC, based on its experimental *in vitro* release

Table 3
Pharmacokinetic parameters of budesonide-loaded LPP formulations and physical mixtures (budesonide/Lactohale® 200 (5/95)) in rats.

Parameters	C_{max} (μg/l)	T_{max} (min)	AUC (0–6) μg/l*h	MRT (0–6) (h)
Physical mixture	417.6 ± 52.13	14.2 ± 1.1	492.4 ± 41.4	1.6 ± 0.2
LPP-1	236.4 ± 41.8*	11.6 ± 0.9	311.5 ± 35.2*	1.6 ± 0.1
LPP-2	64.2 ± 10.5**,#	27.5 ± 1.5	187.3 ± 19.8**,#	2.5 ± 0.3
LPP-3	82.3 ± 27.1**,#	20.0 ± 1.0	192.5 ± 21.2**,#	2.6 ± 0.2

Note: Values are presented as the mean ± SEM (n = 6).
* $p < 0.01$,
** $p < 0.001$ compared to the physical mixture group;
\# $p < 0.01$ compared to the LPP-1 group.

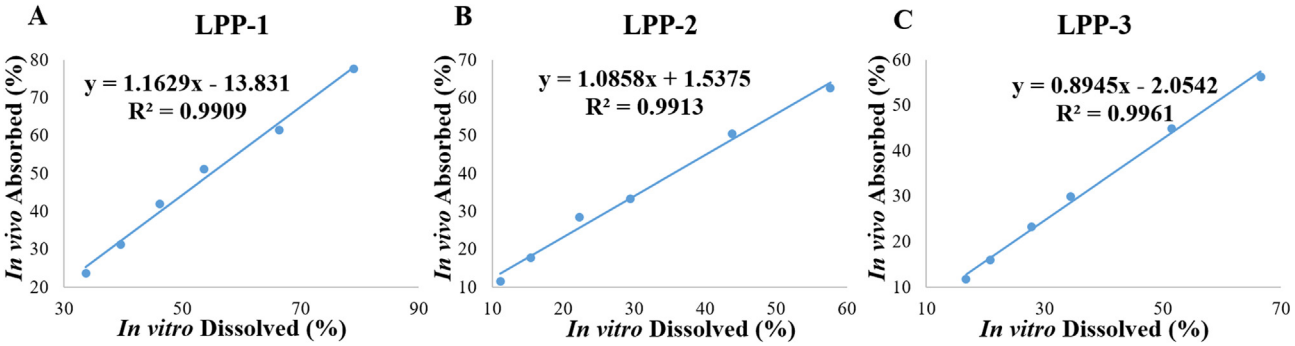

Fig. 9. Linear correlations between the fractions released/dissolved *in vitro* and released/absorbed *in vivo* for LPP-1 (A), LPP-2 (B), and LPP-3 (C), respectively. The straight lines represent linear fits of the experimental data.

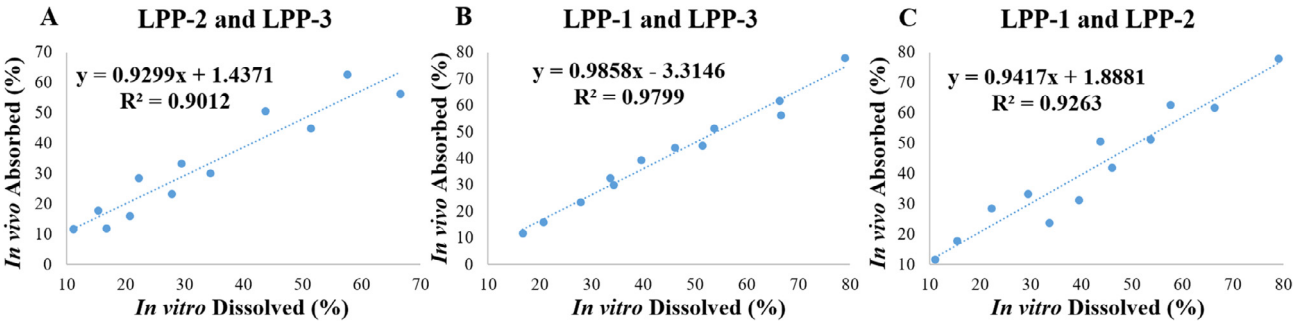

Fig. 10. Level A IVIVC between the fractions released/dissolved *in vitro* and released/absorbed *in vivo* for the three LPPs. (A) IVIVC developed using LPP-2 and LPP-3, (B) IVIVC developed using LPP-1 and LPP-3, and (C) IVIVC developed using LPP-1 and LPP-2. The straight lines represent linear fits of the experimental data.

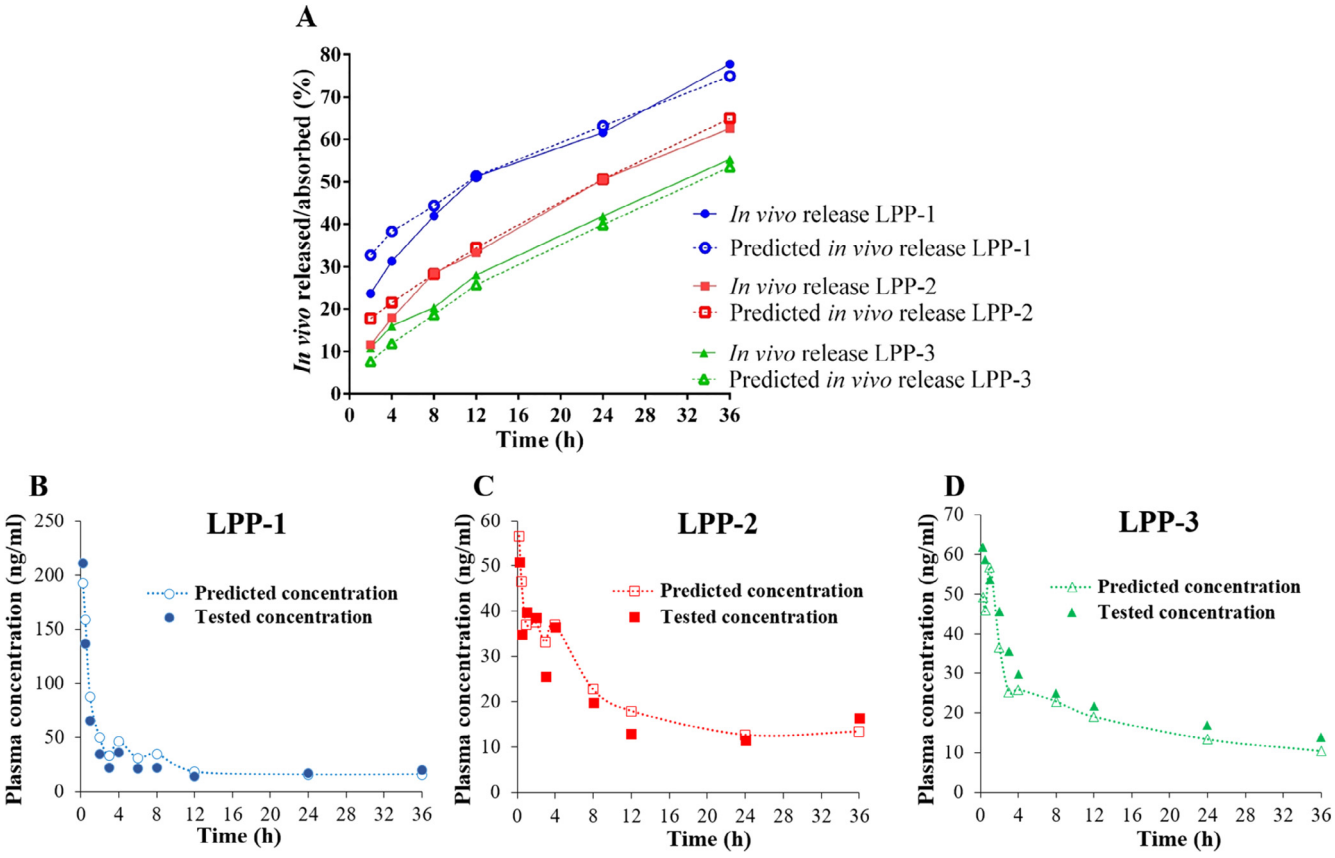

Fig. 11. (A) Experimental and predicted *in vivo* release/absorption profiles of the three LPPs derived from Level A IVIVC. (B-D) Tested plasma concentrations and predicted plasma concentrations convoluted from predicted *in vivo* release/absorption of LPP-1, -2, and -3, respectively.

profile (LPP-1). As shown in Fig. 11A, the predicted *in vivo* release/absorption of each formulation was almost identical to the corresponding *in vivo* release/absorption profile derived from PK data. As a result, a robust IVIVC has been established.

The predictability (prediction error, PE%) of the *in vivo* performance from *in vitro* dissolution of the prepared inhalation formulations with varying release rates (slow, medium, and fast) was validated. According to FDA guidelines of the IVIVC study on extended-release oral dosage forms, internal prediction error should be calculated using the initial data used to develop the IVIVC [11]. As shown in Fig. 11B-D, predicted plasma drug concentrations were convoluted from the predicted *in vivo* release/absorption profiles for the three LPPs, and PE% was calculated for C_{max} and AUC of each formulation. The average absolute value of internal PE% for AUC was 9.48%, 9.56%, and 9.87% for LPP-1, -2, and -3, respectively, while that for C_{max} was 8.66%, 9.67%, and 8.28%, correspondingly. The data indicated that the internal PE% values were all within the range of 10% or less as recommended. Thus, the developed IVIVC could be used to predict the *in vivo* performance of LPPs with equivalent composition from its *in vitro* release characterizations.

3.7. In vivo pharmacodynamics of budesonide-loaded LPPs

The above studies indicated that all the three budesonide-loaded LPP formulations presented sustained release profiles with distinguishable kinetics *in vitro* and *in vivo*. All of them avoided macrophage uptake successfully. To test whether there was a correlation between the *in vitro* behavior and the therapeutic efficacy *in vivo*, the distinct LPP formulations were delivered to the airspace of an established rat model of OVA-induced allergic asthma as planned (Scheme 2). The asthma model group was viewed as a negative control.

Inflammatory markers in the BALF and lung tissues [21] of the drug-administered groups were quantified and compared with those of the asthma model group (Fig. 12 and Supplementary materials, Fig. S1). The total number of inflammatory cells in the BALF was substantially lower after administration of budesonide, especially for LPP-2 and LPP-3 groups ($p < 0.01$ and $p < 0.05$) (Fig. 12A). Moreover, compared to the asthma model group, treatment with LPP-2 and LPP-3 resulted in a significant decrease in the amount of eosinophils and neutrophils ($p < 0.001$ and $p < 0.01$), the most representative inflammatory cell types in asthma. The LPP-1 group did not show a therapeutic effect when compared with the asthma model group ($p > 0.05$).

Interleukin-4 (IL-4) and interleukin-5 (IL-5) are T helper 2 (Th2) cytokines, which play an important role in the inflammatory reaction [22]. Hence, the level of IL-4 and IL-5 in the BALF was considered as a reflection of therapy, and IL-4 and IL-5 mRNA expression in the lung tissues was further measured to verify the results. Compared with the asthma model group, LPP-2 and LPP-3 treatment showed a significant decrease in the concentration and mRNA expression of IL-5 (Fig. 12B-C) and IL-4 (Supplementary materials, Fig. S1A-B). There was no obvious difference between LPP-1 and the asthma model group.

During histopathological evaluation, severe inflammatory cell infiltration around bronchioles and vessels and hyperplasia of goblet cells in the epithelium of airways were observed in the asthma

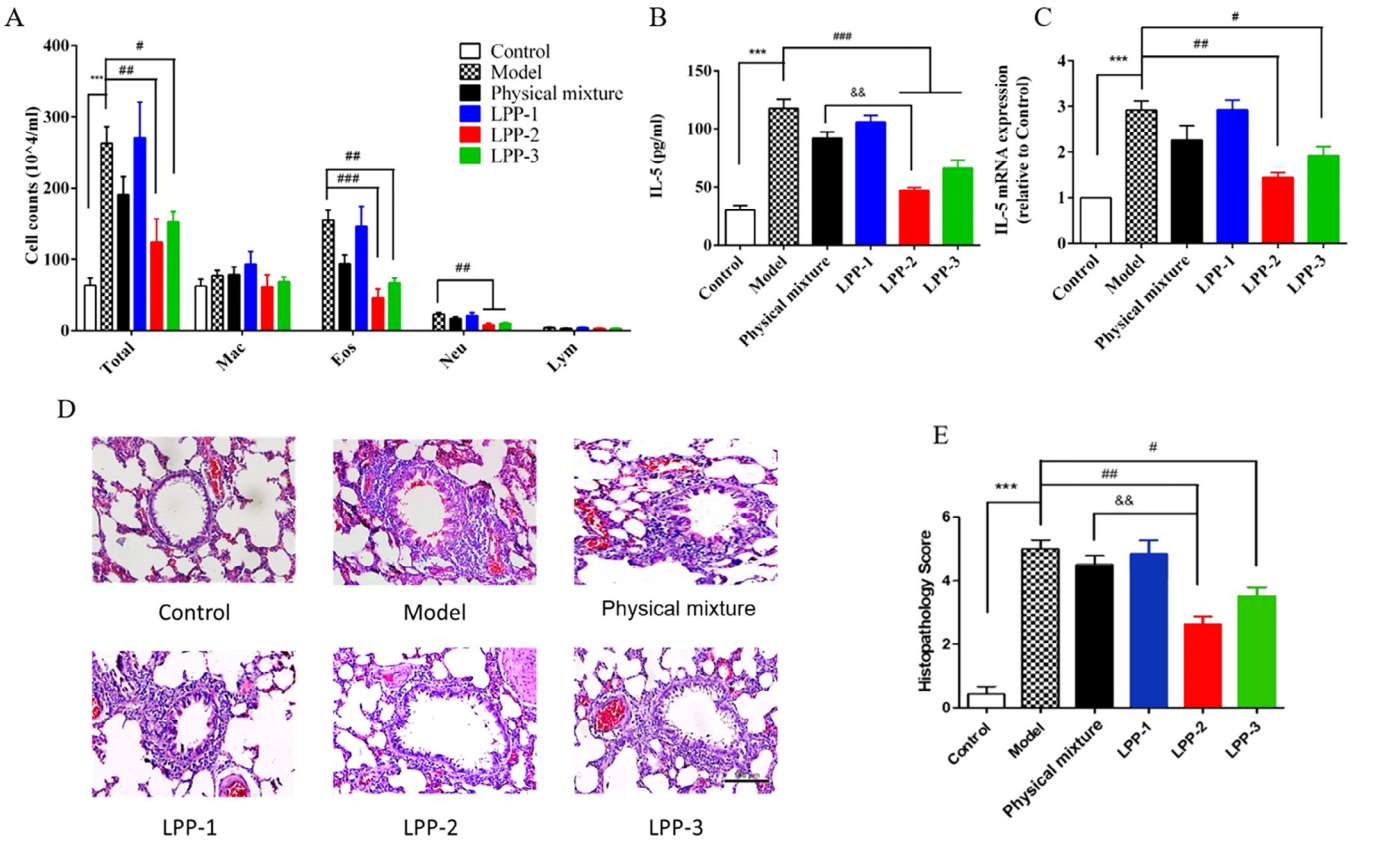

Fig. 12. Therapeutic effect of successive treatment of OVA-induced allergic asthma in rats with budesonide-loaded LPPs. (A) Total white cell count. (B) IL-5 levels in BALF of OVA-sensitized rats measured by ELISA. (C) IL-5 mRNA expression in the lung tissue. (D) Airway inflammation was assessed by hematoxylin and eosin staining of lung sections (original magnification 100×). (E) Total histopathology scores: inflammation was categorized as none (score, 0), mild (score, 1–2), moderate (score, 3–4), or severe (score, 5–6). Values are presented as the mean ± SEM ($n = 5$). Statistics: *** $p < 0.001$ vs. control group. ### $p < 0.001$, ## $p < 0.01$, # $p < 0.05$ vs. Model group, && $p < 0.01$ vs. physical mixture group.

model (Fig. 12D, E). It was shown that treatment with LPP-2 and LPP-3 formulations attenuated the infiltration of inflammatory cells and hyperplasia of goblet cells ($p < 0.01$ and $p < 0.05$). Specifically, the LPP-2 group displayed the maximal level of airway wall thickness attenuation, followed by LPP-3 ($p < 0.01$) (Supplementary materials, Fig. S1C).

4. Discussion

IVIVC is defined as a predictive method, which would shorten the time for pharmaceutical development, save resources, and support biowaivers [23]. Once an IVIVC is established, it can be used to guide formulation and/or process development over various stages of drug product development [24]. However, the number of publications and overall understanding of IVIVC for inhalation products are yet limited. In this aspect, here we attempted to establish the correlations between *in vitro* release and *in vivo* retention/absorption for lung-delivered LPPs.

It has been recommended that two or more formulations with different release characteristics can define an IVIVC [25]. The pores of the LPPs were the tunnels for drug release [26]; thus, its porosity was adjusted by changing the extraction rate of DCM during the solidification of polymer carriers [27] or by premix membrane emulsification [28] to tune the drug release rate. As a result, the three prepared budesonide-loaded LPPs with equivalent composition displayed different release characteristics (slow, medium, and fast release rate) both *in vitro* and *in vivo*. Accordingly, they are suitable for the development of an IVIVC.

The LPPs were prepared to exhibit comparable deposition properties in the deep lung ($MMAD_e$ values of <4 μm) and avoid uncontrollable interferences derived from macrophage uptake, so that more reliable IVIVC could be developed. It has been reported that particles with sizes in the range of 1–3 μm can be easily phagocytized by macrophages [29]. In accordance with this observation, the uptake by macrophages of the physical mixture group (in which particle size of budesonide was approximately 2 μm) was much larger and enlarged in a time-dependent manner. By contrast, LPP formulations ensured a reduced uptake by macrophages *in vitro* (geometric particle sizes were all in the range of 9–20 μm), which was a prerequisite to assure a prolonged residence time in the lungs.

It is under debate whether the PK study should be investigated to assess the fate of drug for lung-delivered formulations, claiming that plasma drug levels might not necessarily represent drug concentrations at the target site or determine the effect [30]. Presently, the European authorities consider plasma concentrations obtained in a PK study to be indicative of the concentrations at the site of action because the plasma concentrations reflect the lung deposition of the drug measured in a compartment downward the lungs [31]. Drugs can be absorbed only from the lung compartment into the systemic circulation, and thus, plasma concentration profiles can provide a variety of information such as pulmonary retention and dissolution character [32].

The *in vivo* absorption rate depends on both the rate of drug release from the formulations and drug permeation across the air/blood barrier. The faster the drug release rate and permeation, the higher is the systemic exposure. According to the Biopharmaceutical Classification System, budesonide is a class II drug with high permeability but low solubility [33]. Hence, the dissolution rate is the rate-limiting step controlling the appearance of budesonide in the plasma [34]. The strategy chosen in this study to obtain high budesonide concentrations in the lung and low systemic exposure was by decreasing the release rate of budesonide. Accordingly, data showed that the shortened retention in the lungs led to larger systemic AUC, which was due to the rapid release characteristics (when comparing LPP-1, -2, and -3). A desirable match between *in vitro* release behavior and *in vivo* systemic exposure was discovered qualitatively.

For IVIVC establishment mathematically, it is essential to assess the *in vivo* absorption profile from the plasma concentration/time data by a mathematical approach [35]. The model-independent deconvolution method with only simple and intuitive operations is recommended by the U.S. Pharmacopoeia, which does not rely on simulating the compartment [36]. In this paper, the method was employed, and acceptable correlations between *in vitro* release and *in vivo* absorption of the three LPPs were established.

Establishing an IVIVC for inhalation dosage forms is always considered extremely challenging owing to their complex nature and the lack of proper *in vitro* release methods mimicking the *in vivo* situation [37,38]. When using sink condition and 5 ml of PBS with pH of 7.3 for drug dissolution, Level A (point-to-point) IVIVC was successfully established, and furthermore, the obtained fitting equation from a combination of two LPPs was demonstrated to be able to accurately predict the *in vivo* performance for the third one, which indicated that the release testing method used here might be suitable for IVIVC development for inhalable LPPs.

The sustained release profiles of LPP-2 and -3 were confirmed by therapeutic outcomes in the allergic asthma rat model. Asthma is caused by chronic inflammation of the airways and characterized by high levels of inflammatory cells in BALF, pathological lung tissues, and thickened airway walls [39]. $CD4^+$ Th2 lymphocytes are central to the disease process and exert their effects through a characteristic repertoire of inflammatory cytokines such as IL-4 and IL-5 [40]. Thus, in our PD study, apart from the inflammatory cell counts, IL-4 and IL-5 levels were viewed as an indicator of therapy. The unsatisfied therapeutic outcomes of LPP-1 and the budesonide/lactose physical mixture (no statistical difference between the two groups) were probably due to the rapid drug release rate accompanied by a high systemic exposure, resulting in insufficient local drug concentration in the lung for the therapeutic effect. The efficacy of LPP-2 and -3 was highlighted by a prolonged residence time in the lungs and a reduced AUC in the plasma. Moreover, owing to the sustained/slower drug release and lower C_{max} in plasma, LPP-2 presented superior antiasthmatic effect to that of LPP-3.

Despite the progress made thus far, there remain some limitations in our present research. For example, the *in vivo* study was carried out only in male SD rats, which should be expanded to different animal models. The number of animal samples was small (e.g., 5 rats per group for PD study) and needed to be enlarged further. In addition, the measurements in the pharmacodynamics study were carried out at single time points. Multipoint measurement was highly desirable in the future study. In addition, the cellular uptake study in primary lung macrophages rather than RAW264.7 macrophage cell line should be investigated. In addition, despite the good correlation between *in vitro* release and *in vivo* absorption for the LPPs, it should be noted that the IVIVC evaluation here was based on animal PK data, and hence, further study on IVIVC using human PK data was required for further confirmation.

5. Conclusions

In this study, budesonide-loaded LPPs with varying *in vitro* release rates were prepared and used to investigate the corresponding *in vivo* behavior after delivery to the airways of rats. LPP-2 with the slowest drug release exhibited the longest lung residence time, lowest systemic exposure, and the best therapeutic efficacy. Level A IVIVC mathematical equation was successfully established using the three budesonide-loaded LPPs to predict

the *in vivo* performance from the *in vitro* fraction dissolved, which could be used for screening desirable budesonide-loaded LPP formulations. Furthermore, *in vitro* release conditions were needed to be further investigated to better mimic the *in vivo* environment. Taken together, our work has set up a longitudinal example of IVIVC establishment in the field of inhalable controlled drug delivery.

Acknowledgments

This project is financially supported by Bayer AG (Germany) and the Major Scientific and Technological Special Projects of National "Major New Drug Discovery" of China (No. 2017ZX09201-002).

Appendix A. Supplementary data

Supplementary data to this article can be found online at https://doi.org/10.1016/j.actbio.2019.06.056.

References

[1] G. Pelaia, A. Vatrella, M.T. Busceti, F. Fabiano, R. Terracciano, M.G. Matera, R. Maselli, Molecular and cellular mechanisms underlying the therapeutic effects of budesonide in asthma, Pulm. Pharmacol. Ther. 40 (2016) 15–21.
[2] I. Sulaiman, L.C. Woei, S.H. Liong, J. Stanslas, Molecularly targeted therapies for asthma: current development, challenges and potential clinical translation, Pulm. Pharmacol. Ther. 40 (2016) 52–68.
[3] S. Chennakesavulu, A. Mishra, A. Sudheer, C. Sowmya, E. Bhargav, Pulmonary delivery of liposomal dry powder inhaler formulation for effective treatment of idiopathic pulmonary fibrosis, Asian J. Pharm. Sci. 13 (2018) 91–100.
[4] A.M. Alonso, S. Saglani, Mechanisms mediating pediatric severe asthma and potential novel therapies, Front. Pediatr. 5 (2017) 154–160.
[5] Z. Liang, R. Ni, J. Zhou, S. Mao, Recent advances in controlled pulmonary drug delivery, Drug Discov. Today 20 (2015) 380–389.
[6] D.A. Edwards, J. Hanes, G. Caponetti, J. Hrkach, A. Benjebria, M.L. Eskew, J. Mintzes, D. Deaver, N. Lotan, R. Langer, Large porous particles for pulmonary drug delivery, Science 276 (1997) 1868–1871.
[7] R. Ni, U. Muenster, J. Zhao, L. Zhang, E.M. Becker-Pelster, M. Rosenbruch, S. Mao, Exploring polyvinylpyrrolidone in the engineering of large porous PLGA microparticles via single emulsion method with tunable sustained release in the lung: in vitro and in vivo characterization, J. Control. Release 249 (2017) 11–22.
[8] C.J. Cheng, L.Y. Chu, R. Xie, Preparation of highly monodisperse W/O emulsions with hydrophobically modified SPG membranes, J. Colloid Interface Sci. 300 (2006) 375–382.
[9] J. Ferin, D.P. Penney, Pulmonary retention of ultrafine and fine particles in rats, Am. J. Respir. Cell Mol. Biol. 6 (1992) 535–542.
[10] P.R. Robinson, L.W. Rees, J. Maddock, A sensitive method for the determination of budesonide in plasma using LC-MS-MS(API), Spec. Publ. R. Soc. Chem. 226 (1998) 88–89.
[11] S. Suarez-Sharp, M.L.J. Duan, H. Shah, P. Seo, Regulatory experience with In Vivo In Vitro Correlations (IVIVC) in new drug applications, AAPS J. 18 (2016) 1–12.
[12] P. Yue, Application of numerical convolution in in vivo/in vitro correlation research, Acta Pharm. Sin. 44 (2009) 19–24.
[13] C.P. Hu, Y.Q. Zou, J.T. Feng, X.Z. Li, The effect of unilateral adrenalectomy on transformation of adrenal medullary chromaffin cells in vivo: a potential mechanism of asthma pathogenesis, PLoS One 7 (2012) 44–56.
[14] Y.H. Chen, R. Wu, B. Geng, Y.F. Qi, P.P. Wang, W.Z. Yao, C.S. Tang, Endogenous hydrogen sulfide reduces airway inflammation and remodeling in a rat model of asthma, Cytokine 45 (2009) 117–123.
[15] J.J. Zou, Y.D. Gao, S. Geng, Role of STIM1/Orai1-mediated store-operated Ca^{2}+ entry in airway smooth muscle cell proliferation, J. Appl. Physiol. 110 (2011) 1256–1263.
[16] K.S. Konduri, S. Nandedkar, N. Düzgünes, V. Suzara, J. Artwohl, R. Bunte, P.R. Gangadharam, Efficacy of liposomal budesonide in experimental asthma, J. Allergy Clin. Immunol. 111 (2003) 321–327.
[17] S. Mao, Y. Shi, L. Li, J. Xu, A. Schaper, T. Kissel, Effects of process and formulation parameters on characteristics and internal morphology of poly(d, l-lactide-co-glycolide) microspheres formed by the solvent evaporation method, Eur. J. Pharm. Biopharm. 68 (2008) 214–223.
[18] C.J. Musante, J.D. Schroeter, J.A. Rosati, T.M. Crowder, A.J. Hickey, Factors affecting the deposition of inhaled porous drug particles, J. Pharm. Sci. 91 (2010) 311–320.
[19] S.W. Oh, H.J. Bang, S.T. Myung, Y.C. Bae, S.M. Lee, The Effect of morphological properties on the electrochemical behavior of high tap density C-$LiFePO_4$ prepared via coprecipitation, J. Electrochem. Soc. 155 (2008) 414–420.
[20] R. Gilibili, B. Murali, In vitro stimulation of multidrug resistance-associated protein 2 function is not reproduced in vivo in rats, Pharmaceutics 10 (2018) 3–11.
[21] N.P. Adams, P.W. Jones, The dose-response characteristics of inhaled corticosteroids when used to treat asthma: an overview of Cochrane systematic reviews, Respir. Med. 100 (2006) 1297–1306.
[22] Jayaprakasam Bolleddula, Ming-Chun Yang, Wang Rong, Goldfarb Joseph, Sampson Hugh, Constituents of the anti-asthma herbal formula ASHMITM synergistically inhibit IL-4 and IL-5 secretion by murine Th2 memory cells, and eotaxin by human lung fibroblasts in vitro, J. Integr. Med. 11 (2013) 195–205.
[23] G. Balan, P. Timmins, D.S. Greene, P.H. Marathe, In vitro–in vivo correlation (IVIVC) models for metformin after administration of modified-release (MR) oral dosage forms to healthy human volunteers, J. Pharm. Sci. 90 (2001) 1176–1185.
[24] S. Jie, D.J. Burgess, In vitro-in vivo correlation for complex non-oral drug products: Where do we stand?, J Control. Release 219 (2015) 644–651.
[25] S. Hardikar, Establishment of in vivo – in vitro correlation: a cogent strategy in product development process, Indian J. Pharm. Educ. Res. 48 (2014) 66–73.
[26] J.M. Cardot, E. Beyssac, M. Alric, In vitro–in vivo correlation: importance of dissolution in IVIVC, Dissolut. Technol. 14 (2007) 15–19.
[27] H. Malinowski, P. Marroum, V.R. Uppoor, W. Gillespie, H.Y. Ahn, P. Lockwood, J. Henderson, R. Baweja, M. Hossain, Draft guidance for industry extended-release solid oral dosage forms. Development, evaluation and application of in vitro-in vivo correlations, Oxygen Trans. Tissue 423 (1997) 269–288.
[28] W. Schloegl, V. Marschall, M.Y. Witting, E. Volkmer, I. Drosse, U. Leicht, M. Schieker, M. Wiggenhorn, F. Schaubhut, S. Zahler, Porosity and mechanically optimized PLGA based in situ hardening systems, Eur. J. Pharm. Biopharm. 82 (2012) 554–562.
[29] S. Mao, J. Xu, C. Cai, O. Germershaus, A. Schaper, T. Kissel, Effect of WOW process parameters on morphology and burst release of FITC-dextran loaded PLGA microspheres, Int. J. Pharm. 334 (2007) 137–148.
[30] H.S. Ribeiro, L.G. Rico, G.G. Badolato, H. Schubert, Production of O/W emulsions containing astaxanthin by repeated premix membrane emulsification, J. Food Sci. 70 (2010) 117–123.
[31] S. Chono, T. Tanino, T. Seki, K. Morimoto, Influence of particle size on drug delivery to rat alveolar macrophages following pulmonary administration of ciprofloxacin incorporated into liposomes, J. Drug Target. 14 (2006) 557–566.
[32] C. Evans, D. Cipolla, T. Chesworth, E. Agurell, R. Ahrens, D. Conner, S. Dissanayake, M. Dolovich, W. Doub, A. Fuglsang, Equivalence considerations for orally inhaled products for local action-ISAM/IPAC-RS European Workshop report, J Aerosol. Med. Pulm. Drug Deliv. 25 (2012) 117–139.
[33] K. Nahar, N. Gupta, R. Gauvin, S. Absar, B. Patel, V. Gupta, A. Khademhosseini, F. Ahsan, In vitro, in vivo and ex vivo models for studying particle deposition and drug absorption of inhaled pharmaceuticals, Eur. J. Pharm. Sci. 49 (2013) 805–818.
[34] N. Grekas, K. Athanassiou, K. Papataxiarchou, S. Rizea Savu, L. Silvestro, Pharmacokinetic study for the establishment of bioequivalence of two inhalation treatments containing budesonide plus formoterol, J. Pharm. Pharmacol. 66 (2014) 1677–1685.
[35] A. Dokoumetzidis, P. Macheras, IVIVC of controlled release formulations: Physiological-dynamical reasons for their failure, J. Control. Release 129 (2008) 76–78.
[36] J.V. Andhariya, J. Shen, S. Choi, Y. Wang, Y. Zou, D.J. Burgess, Development of in vitro-in vivo correlation of parenteral naltrexone loaded polymeric microspheres, J. Control. Release 255 (2017) 27–35.
[37] H.M. Piao, H.J. Cho, E.C. Oh, S.J. Chung, C.K. Shim, D.D. Kim, Budesonide microemulsions for enhancing solubility and dissolution rate, J. Kor. Pharm. Sci. 39 (2009) 417–422.
[38] L.D. Hu, Y. Liu, X. Tang, Q. Zhang, Preparation and in vitro/in vivo evaluation of sustained-release metformin hydrochloride pellets, Biopharmaceutics 64 (2006) 185–192.
[39] M. Johnathan, S.H. Gan, E.M.F. Wan, A.H. Faezahtul, A.A. Nurul, Phytochemical profiles and inhibitory effects of Tiger Milk mushroom (Lignosus rhinocerus) extract on ovalbumin-induced airway inflammation in a rodent model of asthma, BMC Complement. Altern. Med. 16 (2016) 1–13.
[40] S.S. Athari, S.M. Athari, F. Beyzay, M. Movassaghi, E. Mortaz, M. Taghavi, Critical role of Toll-like receptors in pathophysiology of allergic asthma, Eur. J. Pharmacol. 808 (2016) 21–27.